Available online at www.sciencedirect.com

ScienceDirect

Ceramics International 40 (2014) 4251–4256

CERAMICS INTERNATIONAL

www.elsevier.com/locate/ceramint

Structural and electrical properties of BZT-added BNLT ceramics

P. Kantha[a], N. Pisitpipathsin[b], K. Pengpat[b], S. Eitssayeam[b], S. Pojprapai[a,*]

[a]School of Ceramic Engineering, Institute of Engineering, Suranaree University of Technology, Nakhon Ratchasima 30000, Thailand
[b]Department of Physics and Materials Science, Faculty of Science, Chiang Mai University, Chiang Mai 50200, Thailand

Received 7 August 2013; accepted 21 August 2013
Available online 29 August 2013

Abstract

Lead free piezoelectric ceramics $(1-x)$BNLT$-x$BZT with $x=0.00$, 0.06, 0.09 and 0.12 were prepared using a two-step mixed oxide method. Dielectric, ferroelectric and piezoelectric properties of the ceramics were improved by the addition of the BZT. XRD results show tetragonal symmetry structure of the BNLT–BZT ceramics. It was found that the tetragonality increases with increasing BZT content. The optimum composition is $x=0.09$, where the maximum values of the piezoelectric constant d_{33} ($\sim$126 pC/N) and dielectric constant ($\sim$2400) were obtained at room temperature. This BNLT–BZT system can be a promising candidate for lead-free piezoelectric ceramics.

Keywords: C. Dielectric properties; C. Piezoelectric properties; D. Perovskites; D. $BaTiO_3$ and titanates

1. Introduction

Lead-based piezoelectric materials are a source of pollution in electronic industrial applications and mostly come from the production of $Pb(Zr,Ti)O_3$ (PZT), $PbTiO_3$ (PT) and $Pb(Mg_{1/3}Nb_{2/3})O_3$ (PMN) compounds. Many researchers have focused on finding alternative piezoelectric materials containing no lead [1–6]. Bismuth sodium titanate (BNT: $(Bi_{0.5}Na_{0.5})TiO_3$) based materials have been of particular interest in the field of piezoelectric materials and devices for the past few decades [7–9]. BNT crystals have a perovskite structure with rhombohedral symmetry at room temperature and two phase transitions at T_2 ($\sim$220 °C) and T_m ($\sim$320 °C) where ferroelectric (FE) rhombohedral changes to antiferroelectric (AF) tetragonal, and AF tetragonal changes to paraelectric (PA) cubic, respectively. However, the drawback of BNT ceramics is the difficulty in poling due to high conductivity. This may be attributed to mobile ions (Na^+, Bi^{3+}) which diffuse easily in the material when an electric field is applied during the poling process, especially at elevated temperatures. Consequently, the dipole moments cannot be completely aligned along the direction of the applied electric field. This results in less the polarization of the material and poor piezoelectric and ferroelectric properties. This problem can be solved by doping A-site and B-site cations in BNT crystals. Recently, many works showed the improvement of piezoelectric and ferroelectric properties due to the effect of dopants in BNT-based materials such as BNLT [10], BNT–BT [11–13], BNT–BZT [14,15], BNT–KN [1,16] and BNT–BT–KNN [17]. In addition to BNT-based ceramics, barium zirconium titanate ($BaZr_xTi_{1-x}O_3$: BZT) solid solution has been investigated to develop high-quality lead-free ceramics because of its high dielectric constant and low loss [18]. The substitution of Zr^{4+} ions by the Ti^{4+} ions in $BaTiO_3$ significantly improves the overall electrical properties of the material due to its better chemical stability [19]. It is known that the ferroelectric phase transition temperature of BZT changes with Zr^{4+} content. If x content is more than 10 mol%, BZT ceramics exhibit relaxor behavior [20] while the x content is less than 10 mol%, the BZT ceramics exhibit normal ferroelectric behavior [21]. Recently, Yu et al. reported that $Ba(Zr_{0.05}Ti_{0.95})O_3$ exhibited relatively high piezoelectric and ferroelectric properties (e.g. 236 pC/N) compared to other lead-free ferroelectric materials [22]. In this present work, we aim to study the ferroelectric, piezoelectric and dielectric properties of $(1-x)$BNLT$-x$BZT with $x=0.00$, 0.06, 0.09 and 0.12. To improve the electrical properties of BNLT–BZT ceramics, the ceramics were prepared by using

*Corresponding author. Tel.: +66 44 224542.
E-mail address: soodkhet@sut.ac.th (S. Pojprapai).

0272-8842/$ - see front matter © 2013 Elsevier Ltd and Techna Group S.r.l. All rights reserved.
http://dx.doi.org/10.1016/j.ceramint.2013.08.089

the two-step mixed oxide method. The comparison between electrical properties of BNLT–BZT and that of BNT–BZT obtained from previous works was reported.

2. Experimental

The starting chemicals for producing the $(1-x)(Bi_{0.4871}Na_{0.4871}La_{0.0172}TiO_3$: BNLT$)-x(BaZr_{0.05}Ti_{0.95}O_3$: BZT) ceramics, where $x=0.0$, 0.06, 0.09 and 0.12, were high purity ($>99.0\%$) powders of bismuth oxide: Bi_2O_3 (Fluka), sodium carbonate: Na_2CO_3 (Riedel-de Haën), lanthanum oxide: La_2O_3 (Fluka), titanium dioxide: TiO_2 (Riedel-de Haën), barium carbonate: $BaCO_3$ (Fluka) and zirconium dioxide: ZrO_2 (Riedel-de Haën). BNLT and BZT powders were prepared separately by calcination at 900 °C and 1250 °C for 2 h, respectively and they were then mixed corresponding to the above formula using the ball-milling method for 24 h with ethanol as a milling media. The dried powders were then sieved to prepare pellets of 10 mm in diameter, which were subsequently sintered between 1075 °C and 1500 °C in an electric furnace and air atmosphere under controlled heating and cooling rates of 5 °C /min for 4 h. Phase identification and microstructure of the resulting ceramics were performed by using an X-ray diffractometer (XRD: Philip X'pert) with Cu K_α radiation and scanning electron microscope (SEM, JEOL JSM5910LV). The mean linear intercept method was used to determine the grain size of each sintered sample. Two circular surfaces of the sintered ceramics were polished and coated with silver paste as electrodes. The room temperature dielectric constant (ε_r) and dielectric loss ($\tan\delta$) of the ceramics were measured at 1–100 kHz using an LCZ meter (HP4276A). After the samples were poled for 15 min at 3.0 and 4.0 kV/mm, the piezoelectric charge constant (d_{33}) was measured by using a piezoelectric-d_{33}-meter (APC product inc. S5865). A Sawyer-Tower circuit was used to measure the hysteresis loop of the ceramic samples at room temperature under an electric field of 7 kV/mm.

3. Results and discussion

The phase formation study of $(1-x)$BNLT$-x$BZT ceramics where $x=0.00$–0.12 was carried out by XRD (see Fig. 1). It is found that each XRD pattern exhibited a pure perovskite phase and no second phases. All diffraction peaks were matched with the perovskite $Bi_{0.4871}Na_{0.4871}La_{0.0172}TiO_3$ phase with rhombohedral structure similar to that of the pure BNLT ceramics found in our previous works [2,3,5] Slight shift in d-spacing and splitting of the peak was observed around 46.5°. This implies that there was a change in the lattice parameters and c/a ratio of these ceramics. The lattice parameters were then calculated by using JADE software (version 6.5). Lattice constants (Å) as a function of BZT content are shown in Fig. 2. From the results, it implies that the fraction of the BZT content affects the crystal structure, tetragonality (c/a ratio) of the BNLT–BZT ceramics (e.g. tetragonality increases with increasing BZT content). This phenomenon can be caused by the substitution of Ba^{2+}, and Zr^{4+} into BNLT crystals. The ionic radii of Bi^{3+}, La^{3+} and Na^+ in the 12 fold coordination

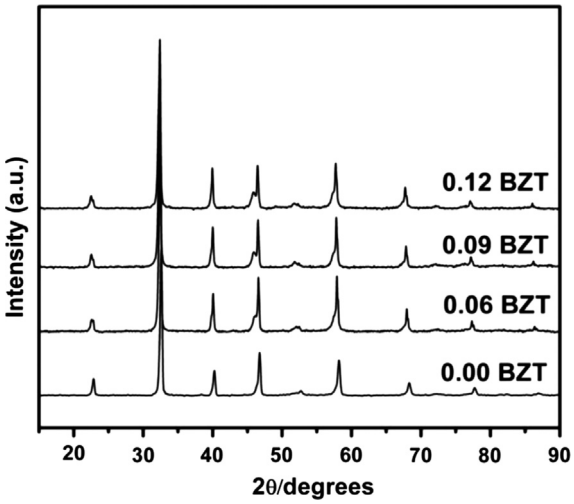

Fig. 1. X-ray diffraction pattern of $(1-x)$BNLT$-x$BZT ceramics where $x=0.0$–0.12.

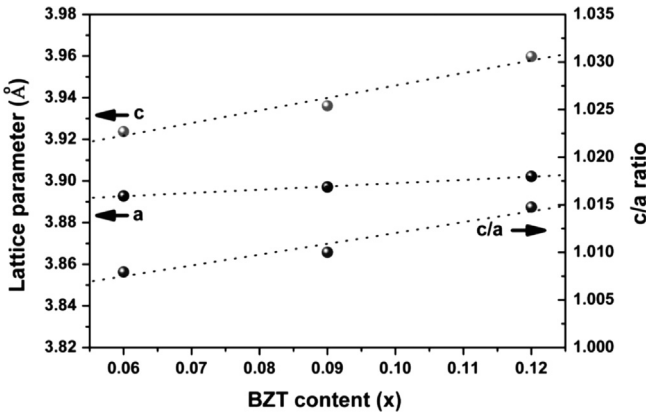

Fig. 2. Lattice parameters and c/a ratio of $(1-x)$BNLT$-x$BZT ceramics where $x=0.0$–0.12.

site and Ti^{4+} in the 6 coordination site for $Bi_{0.4871}Na_{0.4871}La_{0.0172}TiO_3$ perovskite structure were 1.400 Å, 1.360 Å, 1.390 Å and 0.605 Å, respectively. The larger ionic radius Ba^{2+} (1.610 Å) for the 12 fold coordination site and Zr^{4+} (0.720 Å) for the 6 coordination site enter the $Bi_{0.4871}Na_{0.4871}La_{0.0172}TiO_3$ perovskite structure and substitute for the Bi^{3+}, La^{3+}, Na^+ and Ti^{4+} ions, having smaller ionic radii, resulting in the elongation of the crystal structure. Therefore, it can imply that the substitution of Ba^{2+} into the Bi^{3+}, La^{3+}, Na^+ sites and Zr^{4+} into the Ti^{4+} site lead to deformation in lattice parameters and increasing tetragonality. The rhombohedral structure of BNLT ceramics changed continuously into a tetragonal one when the BZT content increased [23].

Fig. 3 shows the as-sintered surface of the $(1-x)$BNLT$-x$BZT ceramics. The microstructure results agree well with the XRD results, as no impurities were observed in the sintered pellets, which exhibited dense microstructures without abnormal grains. Round grains were observed in the pure BNLT ($x=0.0$) and rectangular grains were found in the BNLT–BZT samples. These results indicate that the addition of BZT content has an effect on the morphology of the

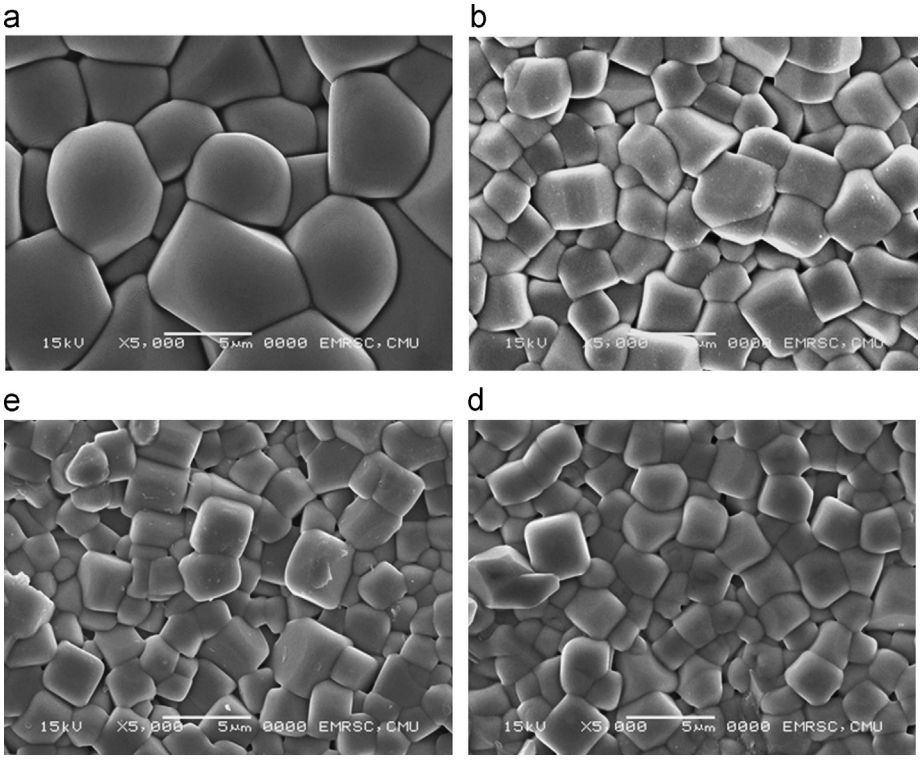

Fig. 3. SEM micrograph of $(1-x)$BNLT$-x$BZT ceramics where (a) $x=0.0$ (BNLT), (b) $x=0.06$, (c) $x=0.09$ and (d) $x=0.12$.

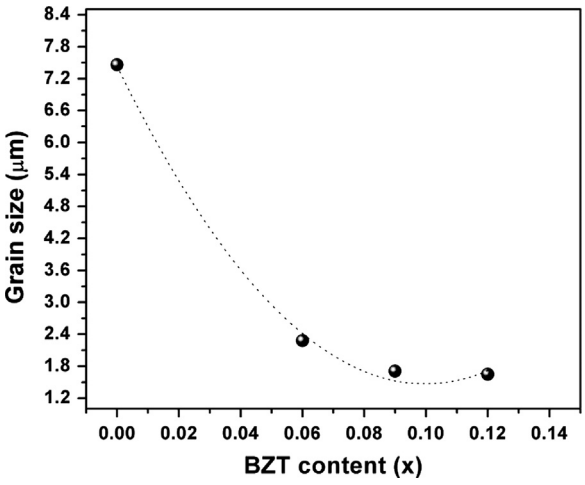

Fig. 4. The relationship between grain size and BZT content of the $(1-x)$ BNLT$-x$BZT ceramics.

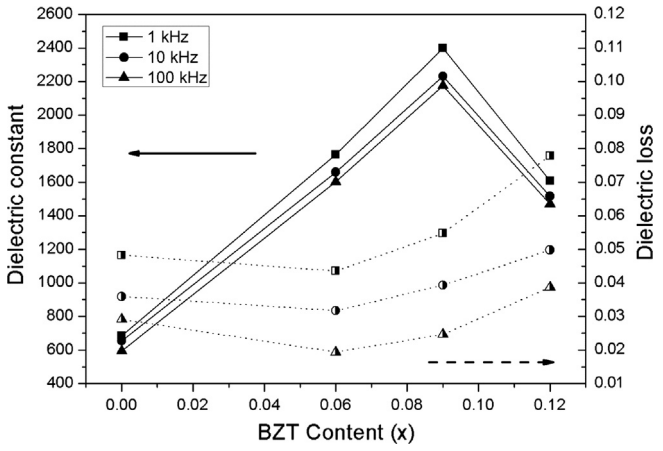

Fig. 5. The dielectric constant and dielectric loss at room temperature as a function of BZT content in $(1-x)$BNLT$-x$BZT system.

microstructure. From microstructural analysis, it was revealed that BZT addition causes a notable decrease in grain size as shown in Fig. 4. The average values of grain sizes, measured by the linear intercept method, decreased from $\sim$7.4 μm for pure BNLT to $\sim$1.5 μm for the $x=0.12$ sample. This is consistent with our previous work [24,25] where the substitution of larger A-site cations Ba^{2+} into the Bi^{3+} site, which possessed a smaller ionic radius, contributed to the inhibition of grain growth.

The dielectric constant (ε_r) of the $(1-x)$BNLT$-x$BZT samples with various frequencies at room temperature is shown in Fig. 5. It can be seen that the BZT addition enhances the dielectric constant of BNLT ceramics. The dielectric constant at 1 kHz was approximately 685 for pure BNLT ($x=0.0$) and increase up to $\sim$2400 at $x=0.09$, then decrease with further BZT addition. These results were partly attributed to ion substitution. In A site, when BZT is added into BNLT, the Ba^{2+} ions replace Na^{+} and act as donor ions. Then, A-site vacancies are created. Chopra et al.[26] reported that if the vacancies were in the lattice, the transfer of atoms would be easier than that in a perfect lattice and the domain wall motion could be induced by a smaller electric field. Thus, the increasing dielectric constant of ceramics was also attributed

to the increment in the magnitude of dipole moment due to the creation of cation vacancies in BNLT–BZT ceramics. However, the decreasing of dielectric constant at $x=0.12$ may be due to the excess of Ba^{2+} ions which replace the La^{3+} and/or Bi^{3+} sites, leading to oxygen vacancies. It is known that oxygen vacancies are the main cause of domain wall clamping which leads to the reduction of dielectric constant [27]. In the other hand, the substitution of Ti^{4+} site by Zr^{4+} ions improves the dielectric constant [14,22]. Low dielectric loss was observed for all samples. These properties may be useful for applications where low loss is particularly needed such as in capacitors and insulators.

The hysteresis loops of the BNLT–BZT ceramics, measured at room temperature using a Sawyer-Tower circuit, are illustrated in Fig. 6. The relevant remanent polarization (P_r) versus the BZT content was then plotted in Fig. 7. For the $x=0.00$ sample (pure BNLT), the hysteresis loop exhibits a typical ferroelectric P–E loop with high remanent polarization while slim hysteresis loops with small remanent polarization were observed for the BZT added samples ($x=0.06$). For $x \geq 0.06$, we observed double hysteresis loops. When BZT content increased, the hysteresis loop became an antiferroelectric-like shape. These results are closely similar to that of our previous study [3] as it was found that double P–E loops are observed in BNLT ceramics with added BT ≥ 6 mol%. This result implies that the anomalies in P–E loops resulted from the transition to an antiferroelectric phase at low temperature after adding BT and/or the electro-mechanical interaction between the polar and non-polar regions, which co-existed in the ceramics [28]. The addition of BZT causes a decrease in the remanent polarization. The same trend was also observed for the value of E_c as shown in Fig. 7. Good ferroelectric properties are generally shown in the sample with high value of the P_r and low value of the E_c. From Fig. 7, the BZT addition in BNLT ceramic with $x=0.06$ caused the reduction of E_c while high P_r was maintained. Therefore, it may be assumed that the 0.94BNLT–0.06BZT system has good ferroelectric properties with a high value of remanent polarization of 30.0 μC/cm^2 and a coercive electric field of 20.8 kV/cm. The low E_c of these samples indicates that the sample can be poled easily because the ferroelectric domains can be reoriented by the low applied field. In addition to P_r and E_c, the characteristics of ferroelectric properties can be qualified by the hysteresis loop squareness (R_{sq}). The R_{sq}

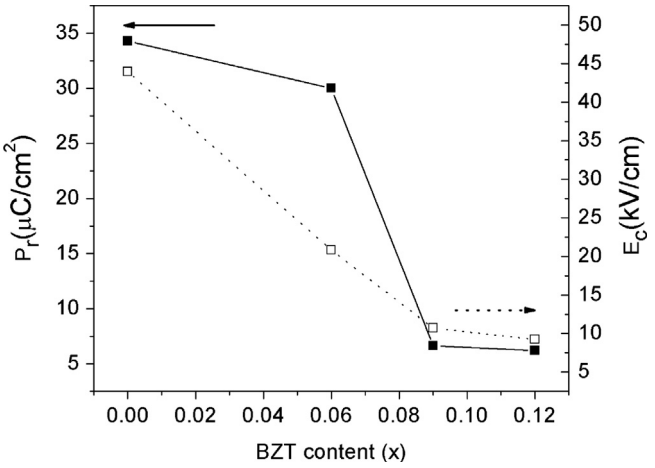

Fig. 7. Room-temperature remanent polarization (P_r) and coercive filed (E_c) as a function of BZT content (x).

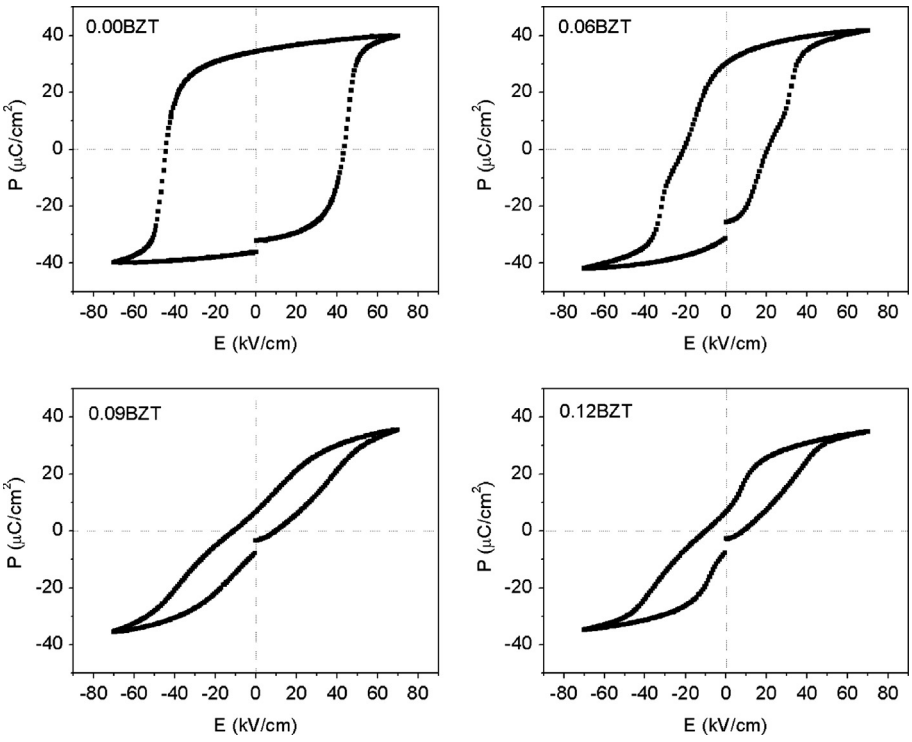

Fig. 6. Hysteresis loop of $(1-x)$BNLT$-x$BZT ceramics at room temperature.

coefficient can be calculate with the equation below [29].

$$R_{sq} = \left(\frac{P_r}{P_s}\right) + \left(\frac{P_{1.1Ec}}{P_r}\right) \quad (1)$$

where P_s is the saturated polarization obtained at some finite field strength below the dielectric breakdown. $P_{1.1Ec}$ is the polarization at the field equal to 1.1Ec. It is known that the ideal square loop, R_{sq} is equal to 2.00 [3]. As listed in Table 1, the loop squareness parameters R_{sq} values of ceramic samples were in the range from 0.26 to 1.55.

To study the piezoelectric property of the samples, the d_{33} piezoelectric coefficient was measured at room temperature using a d_{33}-meter. Two conditions of poling were used in the present work, the samples were poled at 3 kV/mm and 4 kV/mm at 50 °C for 15 min. The measured piezoelectric coefficient as a function of BZT content is shown in Fig. 8. It is seen that the electric field for poling has a strong effect for the d_{33} piezoelectric values, where the higher field gives rise to the higher d_{33} values. In addition, d_{33} values increase with increasing BZT content. For 3 kV/mm poling, the d_{33} value was increased from 71 pC/N for pure BNLT to 76 pC/N for the $x=0.09$ sample, followed by a reduction of d_{33} value to 73 pC/N for the $x=0.12$ sample. The reduction of the d_{33} value for higher BZT content may be due to the difficulty in poling as suggested above.

In case of poling at 4 kV/mm, the d_{33} and piezoelectric voltage coefficient (g_{33}) of the poled $(1-x)$BNLT$-x$BZT ceramics as a function of BZT content are tabulated in Table 1.

Table 1
The electrical properties of the $(1-x)$BNLT$-x$BZT samples.

Composition (X)	ε_r (at 1 kHz)	R_{sq}	d_{33}[a] (pC/N)	g_{33}[a] ($\times 10^{-3}$ Vm/N)
0.00	685	1.55	98	16.2
0.06	1762	0.83	98	6.28
0.09	2400	0.26	126	5.93
0.12	1600	0.29	118	8.33

[a]Poled at 4 kV/mm.

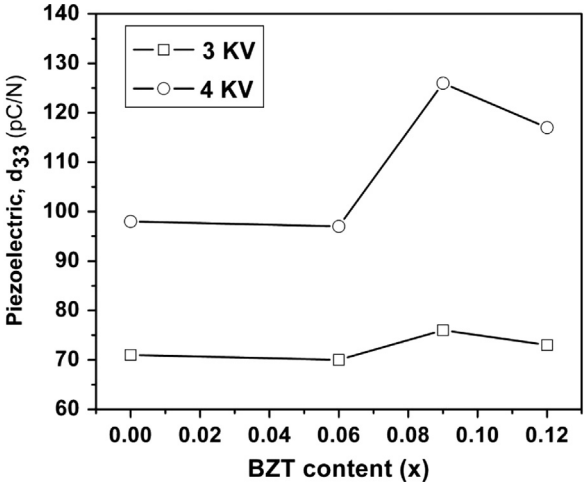

Fig. 8. Piezoelectric coefficient (d_{33}) at 3 and 4 kV of BNLT–BZT ceramics.

Table 2
The important dielectric and piezoelectric properties of the BNLT and 0.91BNLT–0.09BZT samples compared to that of previous works.

Samples	ε_r[a] (T_{room})	tan δ[a] (T_{room})	d_{33} (pC/N)
BNLT (this work)	685 (1 kHz)	0.05 (1 kHz)	98
0.91BNLT–0.09BZT (this work)	2400 (1 kHz)	0.05 (1 kHz)	126
BNLT [10]	550 (1 kHz)	0.04 (1 kHz)	91
0.94BNT–0.06BT [12]	950 (10 kHz)	0.01 (10 kHz)	125
0.91BNT–0.09BZT [14]	~880 (1 kHz)	0.03 (1 kHz)	147

[a]Frequency at 1 kHz.

The coefficient g_{33} was calculated via [30]:

$$g_{33} = \frac{d_{33}}{\varepsilon_0 \varepsilon_r} \quad (2)$$

where ε_0 is the permittivity of free space and ε_r is the relative permittivity. The ε_r was measured at room temperature and shown in Table 1. The significant effect of the d_{33} piezoelectric coefficient was found. The highest piezoelectric constants d_{33} were 126 pC/N and 118 pC/N for 0.91BNLT–0.09BZT and 0.88BNLT–0.12BZT samples, respectively (poled at 4 kV/mm) as compared with that of pure BNLT sample (98 pC/N). The improvement of piezoelectric properties is attributed to the deformation of the BNLT lattice caused by the incorporation of Ba^{2+} ions, which probable substitute Bi^{3+}, Na^{+} or La^{3+} ions at A-sites and/or Zr^{4+} ions, which substitute Ti^{4+} at B-sites of a BNLT perovskite structure. The difference in diameter of replacement ions induced a geometrical deformation of the BNLT lattice. This can lead to greater domain mobility, and therefore the piezoelectric properties are significantly enhanced [31,32].

Some electrical properties of the present work and results from other research groups are listed in Table 2. It should be noted that most of electrical properties of the present samples were enhanced by BZT addition. The optimum properties were observed at $x=0.09$ sample. Although the d_{33} value (126 pC/N) in this work is less than that found by Peng et al. [14] (147 pC/N), dielectric constant of our sample (~2400) was much greater than that found in the previous work (~880). Therefore, the $x=0.09$ sample was selected as the composition with optimum properties for this non-lead based system which offers a wide temperature range to use in electronic applications as an environmentally friendly piezoelectric material.

4. Conclusion

In the present work, $(1-x)$BNLT$-x$BZT ceramics with $x=0.00$, 0.06, 0.09 and 0.12 were prepared using a two-step mixed oxide method and a normal sintering technique. A perovskite phase with the mixing of rhombohedral and tetragonal symmetries was observed in all of the BNLT–BZT samples. BZT addition enhanced dielectric constant (ε_r) of BNLT ceramics while low dielectric loss (tan δ) remained. Furthermore, the d_{33} piezoelectric coefficient was improved by the BZT addition. Hysteresis loop of BNLT ceramics exhibited

a typical ferroelectric P–E loop and then deformed to antiferroelectric-like shape with increasing BZT content. The optimum composition for lead-free ferroelectric ceramics is $x=0.06$ because it has good ferroelectric properties with a high value of remanent polarization of 30.0 μC/cm^2 and a low coercive electric field of 20.8 kV/cm. However, the optimum composition for the lead-free piezoelectric ceramics is $x=0.09$, where the maximum values of the piezoelectric constant ($d_{33}\sim126$ pC/N) and dielectric constant ($\varepsilon_r\sim2400$ at 1 kHz) at room temperature were obtained.

Acknowledgments

The authors are thankful to financial support from SUT Research and Development Fund, Suranaree University of Technology.

References

[1] N. Pisitpipathsin, W. Koontasing, S. Eitssayeam, U. Intatha, G. Rujijanagul, K. Pengpat, T. Tunkasiri, Morphotropic phase boundary of lead-free piezoelectric ceramics from BNT–KN system, Advanced Materials Research 55-57 (2008) 225–228.

[2] P. Kantha, K. Pengpat, P. Jarupoom, U. Intatha, G. Rujijanagul, T. Tunkasiri, Phase formation and electrical properties of BNLT–BZT lead-free piezoelectric ceramics system, Current Applied Physics 9 (2009) 460–466.

[3] N. Pisitpipathsin, K. Pengpat, P. Kantha, W. Leenakul, S. Eitssayeam, G. Rujijanagul, T. Tunkasiri, Dielectric properties of lead-free solid solution of $Bi_{0.487}Na_{0.487}La_{0.017}TiO_3$–$BaTiO_3$, Phase Transitions 83 (2010) 875–883.

[4] N. Pisitpipathsin, P. Kantha, K. Pengpat, G. Rujijanagul, Influence of Ca substitution on microstructure and electrical properties of $Ba(Zr,Ti)O_3$ ceramics, Ceramics International 39 (Suppl. 1) (2013) S35–S39.

[5] P. Kantha, N. Pisitpipathsin, K. Pengpat, Enhanced electrical properties of lead-free BNLT–BZT ceramics by thermal treatment technique, Ceramics International 39 (Suppl. 1) (2013) S59–S63.

[6] J. Rodel, W. Jo, K.T.P. Seifert, E.M. Anton, T. Granzow, Perspective on the development of lead-free piezoceramics, Journal of the American Ceramic Society 92 (2009) 1153–1177.

[7] Q. Xu, X. Chen, W. Chen, S. Chen, B. Kim, J. Lee, Synthesis, ferroelectric and piezoelectric properties of some $(Na_{0.5}Bi_{0.5})TiO_3$ system compositions, Materials Letters 59 (2005) 2437–2441.

[8] D.Z. Jin, X.M. Chen, Z.C. Xu, Influence of dispersed coarse grains on mechanical and piezoelectric properties in $(Bi_{1/2}Na_{1/2})TiO_3$ ceramics, Materials Letters 58 (2004) 1701–1705.

[9] H. Nagata, T. Takenaka, Additive effects on electrical properties of $(Bi_{1/2}Na_{1/2})TiO_3$ ferroelectric ceramics, Journal of the European Ceramic Society 21 (2001) 1299–1302.

[10] A. Herabut, A. Safari, Processing and electromechanical properties of $(Bi_{0.5}Na_{0.5})_{(1-1.5x)}La_xTiO_3$ ceramics, Journal of the American Ceramic Society 80 (1997) 2954–2958.

[11] T. Takenaka, K. Sakata, K. Toda, Acoustic wave characteristics of lead-free $(Bi_{1/2}Na_{1/2})_{0.99}Ca_{0.01}TiO_3$ piezoelectric ceramic, Japanese Journal of Applied Physics (Suppl. 28-2) (1989) 59–62.

[12] T. Takenaka, K. Maruyama, K. Sakata, $(Bi_{1/2}Na_{1/2})TiO_3$–$BaTiO_3$ system for lead-free piezoelectric ceramics, Japanese Journal of Applied Physics 30 (1991) 2236–2239.

[13] R. Dittmer, K.G. Webber, E. Aulbach, W. Jo, X. Tan, J. Rodel, Electric-field-induced polarization and strain in $0.94(Bi_{1/2}Na_{1/2})TiO_3$–$0.06BaTiO_3$ under uniaxial stress, Acta Materialia 61 (2013) 1350–1358.

[14] C. Peng, J.F. Li, W. Gong, Preparation and properties of $(Bi_{1/2}Na_{1/2})TiO_3$–$Ba(Ti,Zr)O_3$ lead-free piezoelectric ceramics, Materials Letters 59 (2005) 1576–1580.

[15] B. Parija, T. Badapanda, S.K. Rout, L.S. Cavalcante, S. Panigrahi, E. Longo, N.C. Batista, T.P. Sinha, Morphotropic phase boundary and electrical properties of $1-x[Bi_{0.5}Na_{0.5}]TiO_3$–$xBa[Zr_{0.25}Ti_{0.75}]O_3$ Lead-free piezoelectric ceramics, Ceramics International 39 (2013) 4877–4886.

[16] H. Ishii, H. Nagata, T. Takenaka, Morphotropic phase boundary and electrical properties of bismuth sodium titanate—potassium niobate solid-solution ceramics, Japanese Journal of Applied Physics 40 (2001) 5660–5663.

[17] J.E. Daniels, W. Jo, J. Rodel, V. Honkimaki, J.L. Jones, Electric-field-induced phase-change behavior in $(Bi_{0.5}Na_{0.5})TiO_3$–$BaTiO_3$–$(K_{0.5}Na_{0.5})NbO_3$: a combinatorial investigation, Acta Materialia 58 (2010) 2103–2111.

[18] S. Mahajan, O.P. Thakur, D.K. Bhattacharya, K. Sreenivas, A comparative study of $Ba_{0.95}Ca_{0.05}Zr_{0.25}Ti_{0.75}O_3$ relaxor ceramics prepared by conventional and microwave sintering techniques, Materials Chemistry and Physics 112 (2008) 858–862.

[19] Y. Zhi, A. Chen, R. Guo, A.S. Bhalla, Dielectric properties and high tunability of $Ba(Ti_{0.7}Zr_{0.3})O_3$ ceramics under dc electric field, Applied Physics Letters 81 (2002) 1285–1287.

[20] P. Kumar, S. Singh, J.K. Juneja, C. Prakash, K.K. Raina, Influence of calcium substitution on structural and electrical properties of substituted barium titanate, Ceramics International 37 (2011) 1697–1700.

[21] F. Moura, A.Z. Simoes, B.D. Stojanovic, M.A. Zaghete, E. Longo J.A. Varela, Dielectric and ferroelectric characteristics of barium zirconate titanate ceramics prepared from mixed oxide method, Journal of Alloys and Compounds 462 (2008) 129–134.

[22] Z. Yu, C. Ang, R. Guo, A.S. Bhalla, Piezoelectric and strain properties of $Ba(Ti_{1-x}Zr_x)O_3$ ceramics, Journal of Applied Physics 92 (2002) 1489–1493.

[23] R.D. Shannon, Revised effective ionic radii and systematic studies of interatomic distances in halides and chalcogenides, Acta Crystallographica Section A 32 (1976) 751–767.

[24] S. Eitssayeam, U. Intatha, G. Rujijanagul, K. Pengpat, T. Tunkasiri, Structural and electrical properties characterization of $(1-x)PbZr_{0.52}Ti_{0.48}O_3$–$xBaFe_{0.5}Nb_{0.5}O_3$ system, Applied Physics A 83 (2006) 295–299.

[25] P. Jarupoom, K. Pengpat, N. Pisitpipathsin, S. Eitssayeam, U. Intatha, G. Rujijanagul, T. Tunkasiri, Development of electrical properties in lead-free bismuth sodium lanthanum titanate–barium titanate ceramic near the morphotropic phase boundary, Current Applied Physics 8 (2008) 253–257.

[26] S. Chopra, S. Sharma, T.C. Goel, R.G. Mendiratta, Structural, dielectric and ferroelectric properties of La doped $PbTiO_3$ sol–gel derived thin films, Ferroelectrics 327 (2005) 97–101.

[27] Y. Xu, Ferroelectric Materials and their Application, Elsevier Science Publishing Company, Inc., New York, 1991.

[28] J. Suchanicz, Behavior of $Na_{0.5}Bi_{0.5}TiO_3$ ceramics in the A.C. electric field, Ferroelectrics 209 (1998) 561–568.

[29] A. Prasatkhetragarn, N. Vittayakorn, S. Ananta, R. Yimnirun, D.P. Cann, Synthesis and dielectric and ferroelectric properties of ceramics in $(1-x)Pb(Zr_{1/2}Ti_{1/2})O_3$–$(x)Pb(Co_{1/3}Nb_{2/3})O_3$ system, Japanese Journal of Applied Physics 47 (2008) 998–1002.

[30] A.J. Moulson, J.M. Herbert, Electroceramics Materials, Properties, Applications, second ed., J. Wiley and Sons, New York, 2003.

[31] X.Y. Zhou, H.S. Gu, Y. Wang, W.Y. Li, T.S. Zhou, Piezoelectric properties of Mn-doped $(Na_{0.5}Bi_{0.5})_{0.92}Ba_{0.08}TiO_3$ ceramics, Materials Letters 59 (2005) 1649–1652.

[32] T. Takenaka, T. Okuda, K. Takegahara, Lead-free piezoelectric ceramics based on $(Bi_{1/2}Na_{1/2})TiO_3$–$NaNbO_3$, Ferroelectrics 196 (1997) 495–498.